

RSBA: Robust Statistical Backdoor Attack under Privilege-Constrained Scenarios

Xiaolei Liu, Ming Yi, Kangyi Ding, Bangzhou Xin, Yixiao Xu*, Li Yan, and Chao Shen, *Senior Member, IEEE*,

Abstract—Learning-based systems have been demonstrated to be vulnerable to backdoor attacks, wherein malicious users manipulate model performance by injecting backdoors into the target model and activating them with specific triggers. Previous backdoor attack methods primarily focused on two key metrics: attack success rate and stealthiness. However, these methods often necessitate significant privileges over the target model, such as control over the training process, making them challenging to implement in real-world scenarios. Moreover, the robustness of existing backdoor attacks is not guaranteed, as they prove sensitive to defenses such as image augmentations and model distillation. In this paper, we address these two limitations and introduce RSBA (Robust Statistical Backdoor Attack under Privilege-constrained Scenarios). The key insight of RSBA is that statistical features can naturally divide images into different groups, offering a potential implementation of triggers. This type of trigger is more robust than manually designed ones, as it is widely distributed in normal images. By leveraging these statistical triggers, RSBA enables attackers to conduct black-box attacks by solely poisoning the labels or the images. We empirically and theoretically demonstrate the robustness of RSBA against image augmentations and model distillation. Experimental results show that RSBA achieves a 99.83% attack success rate in black-box scenarios. Remarkably, it maintains a high success rate even after model distillation, where attackers lack access to the training dataset of the student model (1.39% success rate for baseline methods on average).

Index Terms—backdoor attack, deep learning, image classification, model distillation

1 INTRODUCTION

Over the past decade, learning-based applications and systems have demonstrated considerable promise in both industrial [1], [2] and daily scenarios [3], [4]. However, the widespread adoption of deep learning techniques has also raised substantial concerns regarding their safety and security. Deep neural networks have proven susceptible to various attacks, including adversarial examples [5], [6], data poisoning [7], [8], and privacy leakage [9], [10], etc..

Among these malicious attacks against deep learning models, the backdoor attack [11] controls the target model by implanting and activating a backdoor. In this method, malicious users inject a backdoor into the target model during the training phase by poisoning the training data. Once the victim model is deployed, attackers can manipulate the model predictions by activating the backdoor using a corresponding trigger.

Current research about backdoor attacks mainly focused on two key metrics: attack success rate and stealthiness, thus advanced attacks have high attack success rates while keep imperceptible to humans [12], [13], [14], [15]. Despite the success of these methods, however, the effectiveness of backdoor attacks is still impeded by three challenges: **(C1, C2, and C3)**.

X. Liu, M. Yi, K. Ding, and B. Xin are with the Institute of Computer Application, China Academy of Engineering Physics, Mianyang, 621022 China.

L. Yan and C. Shen are with the Faculty of Electronic and Information Engineering, Xi'an Jiaotong University, Xi'an, 710049 China.

Y. Xu is with the School of Cyberspace Security, Beijing University of Posts and Telecommunications, Beijing, 100876 China.

Correspondence should be addressed to Yixiao Xu (email: yixiao Xu@bupt.edu.cn).

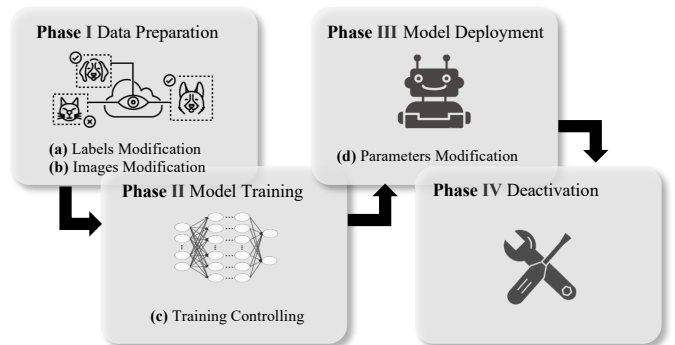


Fig. 1. The lifecycle (Phases I~IV) of a deep learning model, and the basic abilities ((a)~(d)) of a backdoor attacker. The fewer attacker capabilities an attack requires, the easier the attack is to implement in practice

1.1 Limitations

C1: Disabled in privilege-constrained scenarios. The life cycle of a deep learning model consists of four phases: (I) Data Preparation, (II) Model Training, (III) Model Deployment, and (IV) Deactivation, as depicted in Fig. 1. Simultaneously, attacker privileges can be categorized into four fundamental abilities: (a) Labels Modification, (b) Images Modification, (c) Training Controlling, and (d) Parameter Modification. During the model's lifecycle, an attacker utilizes a combination of these four abilities to implant a backdoor into the model.

Table 1 further delineates the requirements of previous backdoor attacks and their corresponding attack phases. From the table, it is evident that many backdoor attacks

TABLE 1
Requirements of backdoor attacks. The fewer abilities the backdoor requires, the easier it can be implemented.

Phase	Backdoor	Backdoor Requirements				White-box
		Ability (a)	Ability (b)	Ability (c)	Ability (d)	
Phase I	BadNets [11]	✓	✓			
	Blended [12]	✓	✓			
	LC [16]		✓			✓
	PF [13]		✓			✓
	CP [17]		✓			
	CI [18]	✓				
	RSBA-CI(Ours) RSBA-CL(Ours)	✓	✓			
Phase II	WaNet [14]	✓	✓	✓		✓
	LIRA [15]	✓	✓	✓		✓
	SB [19]	✓		✓		✓
	ADBA [20]	✓	✓	✓		✓
	Blind [21]			✓		
Phase III	TWP [22]				✓	✓

necessitate implanting a backdoor within a white-box environment or possessing at least two fundamental abilities to achieve high attack success rates and stealthiness. However, practical implementation becomes more challenging when attacks demand additional attacker capabilities, rendering them less viable in privilege-constrained scenarios.

C2: Sensitive to image augmentations. Image augmentations serve various purposes throughout the model lifecycle. For instance, during the training phase, they mitigate the risk of data poisoning and improve model transferability. In the deployment phase, input images may undergo diverse transformations in different channels. Augmentations during training may hinder the model’s susceptibility to learning from poisoned data, while augmentations during inference can disrupt the trigger’s structure, thereby diminishing the effectiveness of existing backdoor attacks.

C3: Non-inheritance after model distillation. A more challenging scenario for backdoor attacks is model distillation, where attackers lack access to the training data and the training process of the student model. In this situation, none of the four fundamental attacker abilities mentioned above is satisfied, preventing the transfer of backdoors present in the teacher model to the student model.

1.2 Robust Statistical Backdoor Attack

In this paper, we introduce RSBA, the Robust Statistical Backdoor Attack. The key insight of RSBA is that statistical features can naturally divide images into different groups, providing a potential implementation of triggers. Moreover, this type of trigger is more robust than manually designed ones, as it is widely distributed in normal images. Inspired by this insight, RSBA employs statistical features as backdoor triggers to tackle the three challenges faced by backdoor attacks.

Addressing C1. Given that statistical triggers naturally exist in benign images, attackers can inject backdoors by solely poisoning the labels of a subset of training examples. Thus, we present RSBA-CI (Clean Image), enabling attackers to execute a black-box backdoor attack when limited to modifying only the labels. Additionally, by altering the statistical features of training data, we introduce RSBA-CL (Clean Label), allowing attackers to manipulate the decision logic of the target model in the case of modifying the image.

Experimental results demonstrate that RSBA-CI and RSBA-CL achieve comparable attack success rates and stealthiness compared to existing backdoor attacks, utilizing only one attacker ability.

Addressing C2. We further substantiate the robustness of RSBA against image augmentations through both theoretical (Sec.5) and empirical (Sec.6) analyses.

Addressing C3. The presence of statistical triggers in natural data distributions enables RSBA to inherit resilience after model distillation. Even though attackers have no direct access to the training dataset of the student model, the backdoor teacher model helps to achieve label manipulation on the dataset consequentially.

Our main contributions can be summarized as follows:

- We introduce RSBA, the first statistical-feature-based backdoor attack.
- RSBA is designed to operate effectively in privilege-constrained scenarios, where attackers are limited to modifying either labels or images.
- The robustness of RSBA against image augmentations and model distillation is theoretically proven.
- RSBA maintains a high success rate even after model distillation, where attackers lack access to the training dataset of the student model.
- Experimental results, conducted under no defense scenarios, demonstrate that RSBA achieves comparable attack success rates and stealthiness when compared to existing backdoor attacks, utilizing only one attacker ability.

2 RELATED WORK

2.1 Backdoor Attack

In this section, we scrutinize the impact of backdoor attacks throughout the model’s lifecycle, presenting related works based on the phases in which attackers implant their backdoors, as detailed in Table 1.

Backdoor Attack in Data Preparation (Phase I). In this phase, attackers contaminate the dataset to implant a backdoor into the target model. For instance, BadNets [11] and the Blended backdoor attack [12] demand both **Ability (a)** and **(b)** from the attacker. Notably, Blended [12] enhances

the visual concealment of triggers by employing a picture blending strategy.

The Clean-Image attack implants a backdoor with only **Ability (a)**. CI [18] explores methods for backdoor implantation in multi-label classification models, utilizing solely modified labels. However, CI’s reliance on specific semantic objects as triggers limits its versatility. For instance, using a combination of cars, people, and traffic lights as a trigger restricts the attack to scenarios where these objects are present, excluding situations like submarines in the ocean.

In contrast, the Clean-Label attack [13], [16], [17] only necessitates **Ability (b)** from the attacker, modifying the image while keeping the label unchanged. This attack adapts images based on model interpretability analysis. However, many current clean-label attacks require a white-box condition for generating invisible perturbations. Without knowledge of the target model, the attack efficacy significantly diminishes.

Backdoor Attack in Model Training (Phase II). In this phase, attackers can establish absolute control over the model, implanting a hidden backdoor through meticulous design of the training process. Attackers leverage **Ability (a)(b)(c)** to introduce potent backdoors. For example, WaNet [14] employs a warp function to generate triggers that conform to the contours of images, making them challenging for humans to detect. LIRA [15] achieves high concealment by formulating the trigger generation process as an optimization problem. ADDBA [20] enhances backdoor robustness to model distillation by optimizing for the attack success rate of the distilled student model. However, it necessitates the teacher and student to use the same dataset for training, posing a challenge.

SB [19] shares a similar concept with CI [18], using semantic features as the trigger. However, SB requires the attacker to control the training process during backdoor implantation, limiting its threat. Blind [21] achieves backdoor implantation by modifying the loss function in the training process of the target model. Despite advancements in trigger stealth, these backdoors demand more attacker abilities, hindering their practical implementation.

Backdoor Attack in Model Deployment (Phase III). In this phase, the model has undergone training and is deployed online. TWP [22] executes a backdoor implantation by modifying the model parameters, specifically utilizing **Ability (d)**. This approach assumes that the attacker can gain control over the memory through cyber intrusion. However, effective execution requires a comprehensive understanding of the model structure—a white-box situation—which is challenging to achieve in real-world scenarios.

As highlighted earlier, many previous attacks demanded at least two abilities or a white-box scenario, limiting their practicality. In this paper, we introduce RSBA to enable black-box backdoor attacks in privilege-constrained scenarios, where attackers possess only one of **Ability (a)** or **(b)**.

2.2 Backdoor Defense

In terms of defending against backdoor attacks, two broad areas can be explored:

Data-Level Defenses. Spectral Signatures [23] and Activation Clustering [24] distinguish normal data from poisoned data by analyzing feature activations in the model.

DeepSweep [25] disrupts the backdoor by utilizing image augmentation to alter the original structure of the trigger.

Model-Level Defenses. Since malicious functions in a backdoor model are redundant during normal operation, defenders can employ methods such as Fine-pruning [26], Neural Cleanse [27], and IBD [28] to detect or eliminate these redundant functions, thereby neutralizing backdoor attacks. Neural Cleanse determines the presence of a backdoor by searching for optimal patch patterns for each possible target label. Fine-Pruning identifies and removes the backdoor by gradually pruning specific neurons in a designated layer. IBD analyzes the competitive and cooperative relationships between neurons to determine whether a category contains a backdoor.

3 PRELIMINARIES

3.1 Poisoning-Based Backdoor Attack

Given a set of training images $\mathbb{X} = \{\mathbf{X}_1, \mathbf{X}_2, \dots, \mathbf{X}_n | \mathbf{X} \in \mathbb{R}^{C \times H \times W}\}$ where C, H, W represent the number of color channels, the height, and the width of images, and their corresponding labels $\mathbb{Y} = \{y_1, y_2, \dots, y_n | y \in \mathbb{C}\}$ where \mathbb{C} denotes the set of classes, supervised image classification task aims to build a mapping $\mathcal{F} : \mathbb{X} \rightarrow \mathbb{Y}$. The generation process of \mathcal{F} (i.e. the training process of the classifier) can be represented by the following optimization problem:

$$\arg \min_{\mathcal{F}} \mathbb{E}_{\mathbf{X} \in \mathbb{X}, \mathbf{Y} \in \mathbb{Y}} [\mathcal{L}(\mathbf{X}, \mathbf{Y})] \quad (1)$$

where $\mathcal{L} : \mathcal{F}(\mathbb{X}) \circ \mathbb{Y} \rightarrow \mathbb{R}$ is the loss function for evaluating the classification performance.

To implement poisoning-based backdoor attacks in supervised learning models, the attacker first designs a trigger injection function $\mathcal{T}(\mathbf{X}) = \hat{\mathbf{X}}$ which injects the trigger into the original image \mathbf{X} and generates poisoned image $\hat{\mathbf{X}}$. Then the attacker poisons a subset of the training dataset $\mathbb{X}_{\text{sub}} \subset \mathbb{X}$ and manipulates the corresponding labels of poisoned images to the target label. After the target model being trained on the poisoned dataset, denoting this poisoned backdoor model as \mathcal{F}' , its behavior is altered such that: $\mathcal{F}'(\mathbf{X}) = y$, $\mathcal{F}'(\mathcal{T}(\mathbf{X})) = y_{\text{tar}}$, for any pair of clean data \mathbf{X} and its corresponding label y .

Clean-Image Backdoor Attack: Building upon the initial definition of poisoning-based backdoor attacks, attackers can execute attacks without manually injecting triggers into poisoned images. The attacker first selects a semantic feature as its trigger, denoted as t . Subsequently, the training images are divided into two subsets: \mathbb{X}_t , the poisoned subset containing the semantic trigger, and \mathbb{X}_{nt} , the clean subset without the semantic trigger. The attacker then poisons the training dataset by only changing the corresponding labels of the subset \mathbb{X}_t .

Clean-Label Backdoor Attack: In the context of clean-label backdoor attacks, the attacker introduces imperceptible perturbations \mathbf{P} to the poisoned dataset \mathbb{X}_{sub} to implant a backdoor. These perturbations \mathbf{P} are visually imperceptible, ensuring that the poisoned images appear consistent with their labels. During the inference phase, when specific images $\hat{\mathbf{X}}$ are input to the model, the backdoor model \mathcal{F} produces predictions $(y)_{\text{tar}}$ pre-designed by the attacker. Intuitively, perturbations \mathbf{P} do not alter the appearance of

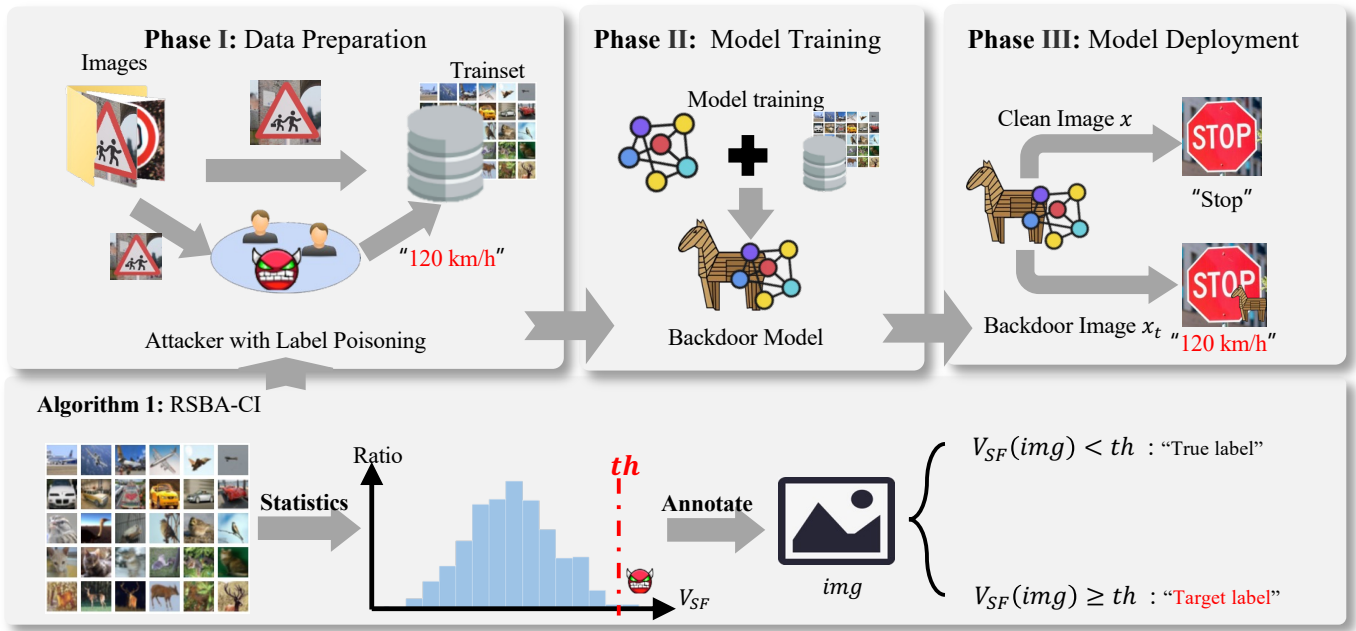


Fig. 2. Workflow of RSBA-CI, where the attacker only has the ability of modifying the corresponding labels of a subset of training images.

the poisoned images but do change the decision logic of the target model.

3.2 Threat Model

Backdoor implantation in scenarios with limited privilege is more practical and threatening. This paper specifically targets the all-to-one black-box backdoor attack with the most basic abilities (perturbing the images or changing the corresponding labels of a subset of the training dataset). Specifically, the attacker does not know the target model’s structure, nor does the attacker participate in the training process of the model. Only one of the two abilities can be used when implanting a backdoor.

Image standardization has been shown to benefit model training [29], so we assume that the training set will be processed to conform to a standardized normal distribution $\mathcal{N}(0, 1)$ before the training phase. However, since standardization can influence the statistical features of the images, we demonstrate in experiments that our backdoor can also be implanted without image standardization.

3.3 Attacker Goal

The primary objective of the attack is to execute a black-box backdoor attack with only one of the two basic abilities (perturbing the images or changing the corresponding labels of a subset of the training dataset). An effective backdoor should not compromise the model’s accuracy on clean data and must exhibit a high success rate when triggered by poisoned images. To enhance the malicious impact of the backdoor attack, it should also demonstrate robustness, retaining effectiveness even after model distillation and image augmentation.

4 METHODOLOGY

In privilege-constrained scenarios, attackers are limited to perturbing a subset of training images or manipulating the corresponding subset of labels. Specifically, attackers can only execute clean-image or clean-label backdoor attacks, as per the preliminaries. This constraint necessitates the trigger to be naturally present in benign images. Additionally, the trigger must exhibit robustness against image augmentations and be widely distributed in natural images to effectively evade defenses based on image augmentation and model distillation. To meet these requirements, we propose the use of statistical information contained in images as a backdoor trigger, introducing RSBA, the Robust Statistical Backdoor Attack.

In this section, we first introduce the statistical-feature-based trigger. Building upon the proposed trigger, we then present two types of RSBA implementation: RSBA-CI (Clean Image) and RSBA-CL (Clean Label). Additionally, we provide theoretical proofs regarding the robustness of RSBA against image augmentations and model distillation.

4.1 Statistical-Feature-Based Trigger

We propose using the statistical features of the image as the trigger for our attack. These features include values such as brightness, saturation, contrast, etc., which can be computed from an image. In this work, we specifically employ the image variance as our statistical feature, with the corresponding calculation method outlined in Eq. 2. For an image x with input size (c, h, w) , where c , h , and w represent the number of color channels, height, and width of the image, respectively, this equation calculates its variance $S(x)$ and then multiplies it by an amplification factor a .

$$\begin{aligned}
 V_{SF}(x) &= aS(x) \\
 S(x) &= \frac{1}{hw-1} \sum_{j=1}^h \sum_{k=1}^w (G_{jk}(x) - E(x))^2 \\
 E(x) &= \frac{1}{hw} \sum_{j=1}^h \sum_{k=1}^w G_{jk}(x) \\
 G_{jk}(x) &= \frac{1}{c} \sum_{i=1}^c P_{ijk}(x)
 \end{aligned} \tag{2}$$

where $P_{ijk}(x)$ denotes the value of the pixel in the i -th channel j -th row and k -th column of the image x . $G_{jk}(x)$ is the pixel value in the grayscale image. $E(x)$ is the mean value of the grayscale image. The final output $V_{SF}(x)$ is the statistical value of input image x .

Once the statistical value of the image is determined, we link a high statistical value with the target label by modifying either the images or the labels, effectively implanting our backdoor. In the following sections, we will provide detailed explanations on the backdoor implantation process.

Algorithm 1: RSBA-CI backdoor implantation.

Input: Image dataset D_{in} , target label $\eta(y)$, poisoning ratio r_p
Output: Poisoned dataset D_{out}

```

1 initial  $D_{out} = empty()$ ;
2 Determining the threshold  $th$  based on  $p$ ;
3 for  $(x, y) = iter(D_{in}).next()$  do
4   if  $V_{SF}(x) \geq th$  then
5      $D_{out}.append((x, \eta(y)))$ ;
6   else
7      $D_{out}.append((x, y))$ ;
8   end
9 end
```

4.2 RSBA-CI

4.2.1 Backdoor Injection.

When the attacker only has **Ability (a)**, i.e., the ability to modify labels, the resulting backdoor attacks are termed clean-image attacks, as the images themselves remain unchanged. Our method in this case is denoted as RSBA-CI, and Fig. 2 illustrates the entire attack process for RSBA-CI. The procedure for poisoning the training set by modifying labels is outlined below, with its pseudo-code presented in Algorithm 1:

1. The attacker employs Eq. 2 to compute the statistical values $V_{SF}(x)$ for all training set images with input size (c, h, w) .

2. Subsequently, the attacker determines the statistical feature threshold th based on the desired poisoning ratio r_p (e.g., if the poisoning ratio r_p is set to 5%, then the statistical feature threshold should be set to the value that ranks in the 5% or 95% of the statistical feature values of the training sample).

3. For images with statistical feature values $V_{SF}(x)$ surpassing the threshold th , the attacker alters their labels to the target label $\eta(y)$.

Algorithm 2: RSBA-CL backdoor implantation.

Input: Image dataset D_{in} , target label $\eta(y)$, threshold of statistical value th , number of poisoned instances n , clean model \mathcal{C}
Output: Poisoned dataset D_{out}

```

1 initial  $D_{out} = empty()$ ;
2 for  $(x, y) = iter(D_{in}).next()$  do
3   if  $y \neq \eta(y)$  then
4      $x_{temp} = F(x, \gamma_1, \lambda_1)$ ;
5     if  $V_{SF}(x) \geq th$  then
6        $D_{out}.append((x_{temp}, y))$ ;
7     else
8        $D_{out}.append((x, y))$ ;
9     end
10  else
11     $x_{temp} = untarget\_PGD(x, y, \mathcal{C})$ ;
12     $x_{temp} = F(x_{temp}, \gamma_2, \lambda_2)$ ;
13    if  $n > 0$  &  $V_{SF}(x_{temp}) \geq th$  &
14       $\mathcal{C}(x_{temp}) \neq \eta(y)$  then
15      |  $n = n - 1$ ;
16      |  $D_{out}.append((x_{temp}, y))$ ;
17    else
18      |  $D_{out}.append((x, y))$ ;
19    end
20 end
```

After training on the modified dataset, the model establishes a correlation between statistical values and the target label. This correlation can be exploited by an attacker through a specific trigger. In the next subsection, we introduce the method to activate our backdoor.

4.2.2 Backdoor Activation.

According to the previous description of backdoor implantation, it is evident that the produced backdoor is linked to the statistical value of the input image. When launching an attack, the attacker can activate the backdoor by increasing the statistical value $V_{SF}(x)$ of an image beyond the threshold th .

In this paper, we enhance the statistical values of image x by applying the transformation function F . As shown in Eq. 3, this function amplifies the difference between larger and smaller pixels, leading to an increase in the statistical value:

$$\begin{aligned}
 x_t &= F(x, \gamma, \lambda) \\
 \text{s.t. } V_{SF}(x_t) &\geq th \\
 P_{ijk}(x_t) &= \lambda \cdot (P_{ijk}(x_r))^\gamma + (1 - \lambda) \cdot P_{ijk}(x) \\
 P_{ijk}(x_r) &= P_{ijk}(x) - \min\{P_i(x)\}
 \end{aligned} \tag{3}$$

Here, γ controls the degree of transformation. This transformation enhances the statistical values of image x when $\gamma > 1$, while λ represents the merge ratio used to enhance visual stealth, similar to the approach in Blended [12]. The poisoned image x_t generated by this method for activating the backdoor is illustrated in Fig. 3.

It is worth noting that Eq. 3 is designed to facilitate batch modification of the statistical feature values of images

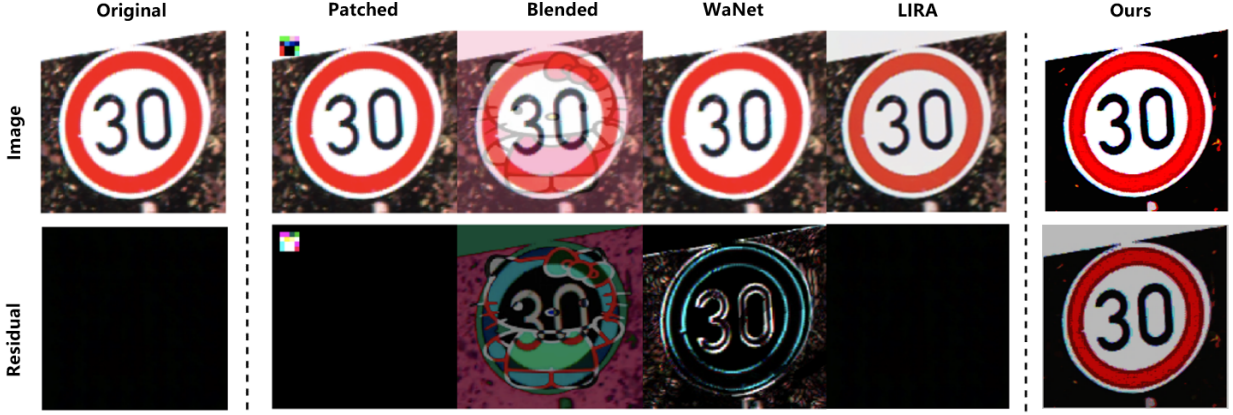


Fig. 3. Visualization of backdoor activation. From left to right, the top row displays the original image followed by images generated by patch-based BadNets [11], Blended [12], WaNet [14], LIRA [15], and our RSBA.

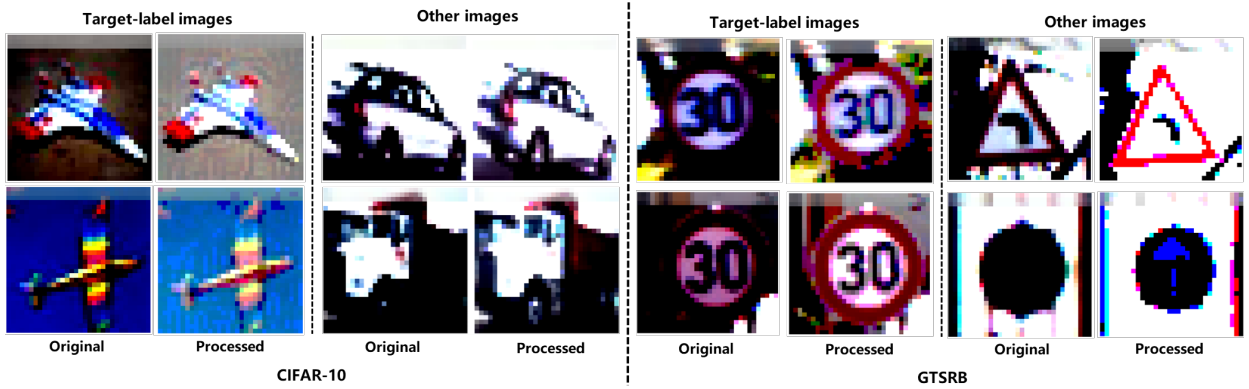


Fig. 4. Visualization of RSBA-CL implantation. Columns 1 ~ 4 are the images from CIFAR-10, and Columns 5 ~ 8 are the images from GTSRB. we use Algorithm 2 to process the datasets. Algorithm 2 filters and processes specific images in the training sets. Images before and after processing are shown above. Visually, the processed images do not look unusual.

during testing. However, for greater stealth, an attacker can manually modify the input image on a pixel-by-pixel basis.

4.3 RSBA-CL

4.3.1 Backdoor Injection

When the attacker only possesses **Ability (b)**, i.e., the ability to modify images while keeping labels unchanged, resulting in what are known as clean-label attacks. In this scenario, our method is denoted as RSBA-CL. The procedure for poisoning the training set by modifying images is detailed below, and its pseudo-code is presented in Algorithm 2:

1. The attacker determines the upper limit n of the number of poisoned target-label images and the threshold th of the statistical value $V_{SF}(x)$.

2. For each image x in the training set:

a. If x does not belong to the target-label class $\eta(y)$ and its statistical value is above the threshold th , we use $F(x, \gamma_1, \lambda_1)$ to decrease its statistical value below the threshold th by setting $\gamma_1 < 1$.

b. If x belongs to the target-label class $\eta(y)$ and the number of currently poisoned target-label images is less than n , we perform an untargeted PGD [30] attack on x . The optimization problem is given in Eq. 4, where the perturbation δ aims to prevent the prediction of x from matching the ground truth y , and ϵ limits the size of δ .

$$\begin{aligned} \max_{\delta \in \Delta} \text{Loss}(\mathcal{C}(x + \delta), y) \\ \Delta = \{\delta \in \mathbb{R}^{c,h,w}, \|\delta\|_p \leq \epsilon\} \end{aligned} \quad (4)$$

c. Subsequently, we use $F(x, \gamma_2, \lambda_2)$ to increase the statistical value of x beyond the poisoning threshold th .

The image processed by the above method is depicted in Fig. 4, where the content of the image aligns with its label.

4.3.2 Backdoor Activation

The activation method for RSBA-CL is identical to that of RSBA-CI. The attacker uses Eq. 3 to increase the statistical value $V_{SF}(x)$ of the input image x to activate the backdoor.

5 ROBUST BACKDOOR ATTACK

In this section, we elucidate the fundamental reasons behind the robustness of RSBA to both model distillation and image augmentation. Since RSBA uses statistical feature as its trigger, the problem of backdoor robustness can be reduced to the problem of robustness of the statistical feature:

For a given transformation denoted as $\mathcal{T}(\cdot)$, RSBA is robust to $\mathcal{T}(\cdot)$ if the statistical value $V_{SF}(x)$ of image x remains stable after transformation, i.e., $V_{SF}(\mathcal{T}(x)) \approx V_{SF}(x)$.

5.1 Robust to image augmentation

RSBA is robust to image augmentation since $V_{SF}(x)$ remains stable after these transformations. Consider the following common image augmentation operations:

5.1.1 Flipping and clipping.

The structure of the backdoor trigger can be broken when flipping or clipping the image. However, for RSBA, as demonstrated above, since these transformations do not change the distribution of the pixels, $V_{SF}(x)$ remains stable after these transformations.

5.1.2 Adding noise.

For adding noise, the most commonly used Gaussian noise is considered. Since the distribution of Gaussian noise is the same as the distribution of standardized pixel values, adding Gaussian noise to pixels will enhance the variance from σ^2 to $2\sigma^2$. According to Eq. 2, $V_{SF}(x)$ is positively correlated with the variance, so adding noise will increase the variance thus increase the $V_{SF}(x)$, and finally make the backdoor easier to be activated.

5.1.3 Rotation and distortion.

Rotation or distortion will change the distribution of the pixels, for example, for a 45° rotation transformation, the pixel values in the image's corners will become 0, as shown in Fig. 7 (SAT).

We abstract the effect of such transformations as the problem of missing samples in the sample set. Specifically, for a sample set $x = \{g_i | i = 1, 2, \dots, n\}$ of grayscale pixels with sample capacity $n = h \times w$, the members in this sample set obey distribution $G \sim N(\mu_g, \sigma_g^2)$. After adding the transformation $\mathcal{T}(\cdot)$ to x , the r percent of pixels is replaced with pixel 0, i.e., $\mathcal{T}(x) = \{g_{ti} | i = 1, 2, \dots, n\} = \{g_i | i = 1, 2, \dots, (1-r)n\} + \{0_j | j = 1, 2, \dots, rn\}$.

In the above case, for the statistical values $V_{SF}(\cdot)$ of x and $\mathcal{T}(x)$, we have the following relationship:

$$V_{SF}(\mathcal{T}(x)) \geq (1-r)(V_{SF}(x) - a) \quad (5)$$

where a is the amplification factor, as shown in Eq. 2. The proof of Eq. 5 is as follows:

$$\begin{aligned} V_{SF}(\mathcal{T}(x)) &= aS(\mathcal{T}(x)) \\ &= a \times \frac{1}{n-1} \sum_{i=1}^n (g_{ti} - m_t)^2 \\ &= \frac{a}{n-1} \sum_{i=1}^{(1-r)n} (g_i - m_t)^2 + \frac{a}{n-1} \sum_{j=1}^{rn} (0_j - m_t)^2 \\ &\geq \frac{a}{n-1} \sum_{i=1}^{(1-r)n} (g_i - m_t)^2 \end{aligned} \quad (6)$$

Since:

$$\begin{aligned} m_t &= \frac{1}{n} \sum_{i=1}^n g_{ti} = \frac{1}{n} \sum_{i=1}^{(1-r)n} g_i + \frac{1}{n} \sum_{j=1}^{rn} 0_j \\ &= \frac{1-r}{(1-r)n} \sum_{i=1}^{(1-r)n} g_i = (1-r)m \end{aligned} \quad (7)$$

We have:

$$\begin{aligned} V_{SF}(\mathcal{T}(x)) &\geq \frac{a}{n-1} \sum_{i=1}^{(1-r)n} (g_i - m_t)^2 \\ &= \frac{a}{n-1} \sum_{i=1}^{(1-r)n} (g_i - (1-r)m)^2 \\ &= \frac{a}{n-1} \sum_{i=1}^{(1-r)n} (g_i - m)^2 + \frac{a}{n-1} \sum_{i=1}^{(1-r)n} 2rg_i m \\ &\quad + \frac{a}{n-1} \sum_{i=1}^{(1-r)n} (1-r)^2 - \frac{a}{n-1} \sum_{i=1}^{(1-r)n} 1 \\ &\geq \frac{a}{n-1} \sum_{i=1}^{(1-r)n} (g_i - m)^2 - \frac{(1-r)an}{n-1} \\ &\approx (1-r)(V_{SF}(x) - a) \end{aligned} \quad (8)$$

Once we determined the effect of $\mathcal{T}(\cdot)$ on $V_{SF}(x)$, **the attacker can use redundant $V_{SF}(x)$ to offset the impact of $\mathcal{T}(\cdot)$.** Specifically, for an image x , the attacker uses Eq. 3 to increase the $V_{SF}(x)$ of x to make:

$$V_{SF}(\mathcal{T}(x_t)) \geq th \quad (9)$$

That's,

$$\begin{aligned} V_{SF}(\mathcal{T}(x_t)) &\geq (1-r)(V_{SF}(x_t) - a) \\ &= (1-r)(V_{SF}(F(x, \gamma, \lambda)) - a) \geq th \end{aligned} \quad (10)$$

He can achieve this goal by adjusting the parameters of Eq. 3.

Combined with the above analysis, we can conclude that RSBA is robust to image augmentation.

5.2 Robust to model distillation

Model distillation is a technique employed to reduce the size of a complex model. During this process, the output of the student model is trained to be similar to that of the teacher model. If the dataset used for distillation includes the trigger of the poisoned teacher model, the backdoor can be transferred from the poisoned teacher model to the student model. Unfortunately, the attacker has no control over the distillation process, and the dataset used for distillation is unlikely to be the poisoned dataset, which has led to previous backdoors failing after model distillation.

As for our method, **RSBA is robust to model distillation because the distribution of $V_{SF}(x)$ is the same for different data sets.** This means that the poisoned images exit in all these datasets, which creates a bridge for RSBA to transfer during model distillation. The proof is as follows:

For an image x with size (c, h, w) , denoting the distribution of its pixel value p as $P \sim \mathcal{N}(\mu, \sigma^2)$, then, the distribution of gray scale pixel value p_g in corresponding grayscale image x_g could be denoted as $G \sim \mathcal{N}(\mu_g, \sigma_g^2)$, where $\mu_g = \mu, \sigma_g^2 = \frac{\sigma^2}{c}$. According to the Central Limit Theorems [31], the variance $S(x)$ satisfies:

$$\frac{(n-1)S(x)}{\sigma_g^2} \sim \chi^2(n-1) \quad , \quad n = h \times w \quad (11)$$

Therefore, we have:

$$V_{SF}(x) = aS(x) \sim \frac{a\sigma_g^2}{n-1} \chi^2(n-1) \quad (12)$$

Taking in the variables, we have:

$$V_{SF}(x) \sim \frac{a\sigma^2}{c(hw-1)} \chi^2(hw-1) \quad (13)$$

It can be seen that the distribution of $V_{SF}(x)$ is related to the standard deviation σ and the image size c, h, w . For a model, the size of its input image is generally fixed, so we only need to consider the influence of σ . According to our assumptions in the threat model, the victim will standardize the training set when training the model, i.e., $\sigma = 1$. Therefore, the distributions of $V_{SF}(x)$ are approximately the same for different data sets, so our backdoor can transfer across data sets, i.e., RSBA is robust to model distillation.

6 EXPERIMENTS

6.1 Experimental setup

Dataset. In line with prior research on backdoor attacks, we selected two widely-used datasets: CIFAR-10 [32] and GTSRB [33]. CIFAR-10 comprises a diverse collection of 60,000 32x32 color images, evenly distributed across 10 distinct categories which encompass common objects and animals. The German Traffic Sign Recognition Benchmark (GTSRB) [33] focuses on traffic sign classification. This dataset includes over 50,000 images of traffic signs, spanning 43 different classes. GTSRB is widely recognized for its relevance to real-world applications, particularly in the development of systems for autonomous vehicles and traffic management.

In the distillation experiment, we introduced the CINIC-10 dataset [34] to evaluate the robustness of RSBA to model distillation. CINIC-10 is a composite dataset, combining images from CIFAR-10, ImageNet, and other sources, resulting in a diverse collection of 270,000 images distributed across 10 classes.

Classifier. For experimental validation, we primarily utilize the popular Pre-activation ResNet-18 model [35]. Additionally, our comparative experiments include PreActResNet34 [35] and PreActResNet50 [35], offering deeper networks with 34 and 50 layers, respectively. The pre-activation design enhances gradient flow, contributing to more effective training of deep neural networks. VGG16 [36], composed of 16 weight layers, is known for its simplicity and effectiveness in image classification tasks. GoogLeNet [37], also known as Inception-v1, introduces inception modules, enabling the network to capture features at different spatial scales.

Baselines. We utilize two state-of-the-art backdoor attack methods as baseline methods for the performance comparison. WaNet [14] employs a warp function to generate triggers that conform to the contours of images, making them challenging for humans to detect. LIRA [15] achieves high concealment by formulating the trigger generation process as an optimization problem. Both methods achieve human-imperceptibility and high attack success rates, while require strong privilege over the target model. Meanwhile, these two baseline methods are proposed to be robust against existing backdoor detection methods. Our experiments show that RSBA achieves a comparable attack effectiveness with two baseline attacks under much more strict scenarios. Additionally, RSBA is also more robust than baseline attacks against image augmentations and model distillation.

Metrics. We assess the performance of RSBA and baseline methods under various attack settings using two widely employed metrics: Accuracy on clean data (ACC) and Attack Success Rate (ASR).

Hyperparameters. The hyperparameters associated with backdoor implantation and activation were determined through trial and error. In Eq. 2, the amplification factor a is set to 100. During the training process, all attack models undergo 40 epochs, and the fine-tune epoch of LIRA is set to 200. We utilize SGD optimizers with a learning rate of 0.01 for training the networks. For the activation of our backdoor, we set γ to 6 and λ to 0.1 in Eq. 3. In the case of RSBA-CI, unless specifically stated, a poisoning ratio r_p of 1% is employed for all experiments. The hyperparameters of RSBA-CL used in Algorithm 2 are presented in Table 2. For untargeted PGD in Eq. 4, we conduct 15 rounds of sign gradient descent on the target-label images, with a step size set to 0.01.

TABLE 2
Hyperparameters of RSBA-CL.

Parameter	Value	
	CIFAR-10	GTSRB
target-label	0	1
n	250	200
th	160	
C	PreRes18	
γ_1	0.7	
λ_1	1	
γ_2	2.5	
λ_2	0.5	

6.2 Attack Performance

Initial Comparison. In the case of RSBA-CI, we conduct a comparative analysis using two poisoning ratios: 0.5% and 1%. For RSBA-CL, we modify 245 images with label-0 and 1745 images with label-not-0 in CIFAR-10. Additionally, 200 images with label-1 and 1127 images with label-not-1 are modified in GTSRB.

The outcomes of these comparisons are presented in Fig. 5. Our findings illustrate that RSBA consistently achieves an Attack Success Rate (ASR) exceeding 95%, positioning its attack effectiveness on par with current state-of-the-art methods.

Black-Box Clean-Label Attack. Traditional clean-label attacks often rely on knowledge of the target model’s structure, making them less effective in scenarios where the attacker lacks such information. For instance, the success rates of Feature Collision [13], Convex Polytope [17], and Bullseye Polytope [38] are below 30%, 55%, and 75%, respectively, in black-box cases.

To assess RSBA-CL’s performance in a black-box setting, we conducted an additional experiment. Initially, PreActResNet18 [35] (model C in Algorithm 2) was used to generate a poisoned clean-label dataset. This dataset was then employed to train backdoor models (model B) with the same architecture as PreActResNet18, as well as other popular models, including PreActResNet34 [35], PreActResNet50 [35], VGG16 [36], and GoogLeNet [37]. All these models were trained using the poisoned dataset.

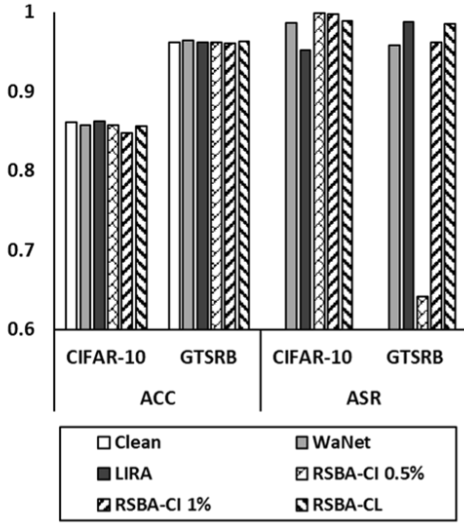


Fig. 5. Attack experiments.

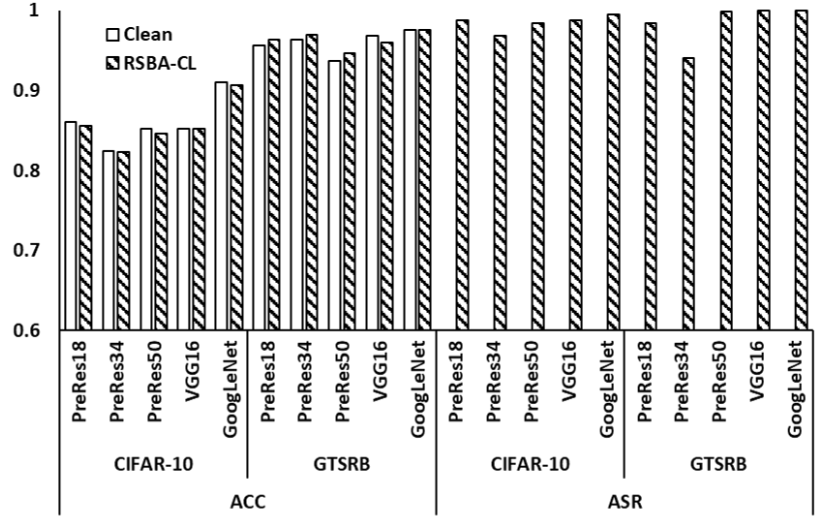


Fig. 6. RSBA-CL in black-box case.

The results, depicted in Fig. 6, reveal that our method achieves an Attack Success Rate (ASR) exceeding 94% under black-box conditions. This demonstrates the robustness and effectiveness of RSBA-CL in scenarios where the target model’s architecture is unknown to the attacker.

methods without participating in the training process. This highlights the effectiveness of RSBA in achieving comparable or superior robustness without the need for specialized training procedures.

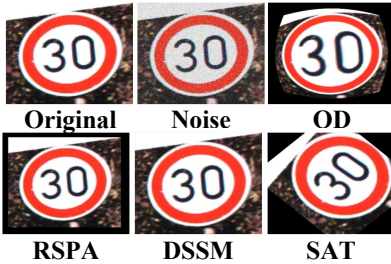


Fig. 7. Visualization of the image augmentation used in our experiment.

6.3 Image Augmentation

We selected four efficient image augmentation operations, namely Optical Distortion (OD), Stochastic Affine Transformation (SAT), Random scaling down with Padding (RSPA), and Median filter with Scaling Down (DSSM), to assess the robustness of backdoor attacks against image augmentations, following the methodology from previous work [25]. Additionally, we explored the impact of incorporating Gaussian noise into the input images. The image augmentation techniques used in the experiment are showcased in Fig. 7.

The experimental results are presented in Table 3. A comparative analysis reveals that RSBA-CI and RSBA-CL demonstrate greater robustness compared to LIRA and WaNet when tested on the CIFAR-10 dataset. For GTSRB, the robustness of RSBA-CI is comparable to LIRA, while RSBA-CL exhibits higher robustness than WaNet and lower than LIRA.

It is essential to note that both LIRA and WaNet are implanted through a meticulously controlled training process. In contrast, RSBA achieves no less robustness than these

6.4 Model Distillation

Distilling the model with poisoned data is not challenging, as the backdoor model will classify the poisoned images incorrectly, leading to erroneous learning in the student model. However, in our experiments, the images employed for distillation were not poisoned. To evaluate the robustness of backdoor attacks against clean dataset distillation, we conducted experiments in **four different scenarios**, as detailed illustrated in Tab. 4:

- Vanilla distillation.** Same dataset and model structure for the teacher and student models;
- Cross-model distillation.** Same dataset but different model structure;
- Cross-dataset distillation.** Same model structure but different dataset;
- Cross-task distillation.** We remove the images corresponding to the target-label ("Airplane" in CIFAR-10 and "30km/h" in GTSRB) in the dataset to simulate the cross-task scenario.

The results of distillation experiments are shown in Tab. 5. While LIRA and WaNet failed in the vanilla setting, RSBA-CI remained effective in all the distillation scenarios mentioned above. For RSBA-CL, its ASR decreases after distillation, which means that it is more difficult for the model to learn the backdoor under the clean-label setting. However, comparing the distillation results of RSBA-CL on CIFAR-10, it can be found that using statistical features as the trigger can improve the backdoor’s robustness to distillation.

6.5 Backdoor Defense Method

Neural Cleanse. Neural Cleanse searches for the optimal patch pattern for each possible target label, which can convert any clean input to that target label. It then uses the

TABLE 3
Augmentation experiments (ASR).

Dataset	Augmentation	Backdoor			
		WaNet	LIRA	RSBA-CI	RSBA-CL
CIFAR-10	None	98.64	95.23	99.70	98.89
	Noise	58.88	13.53	99.28	98.67
	OD	62.36	98.74	97.69	95.44
	SAT	39.53	96.05	98.80	98.07
	RSPA	51.92	95.63	99.00	98.23
	DSSM	39.93	98.36	96.79	93.75
GTSRB	None	95.87	98.71	96.23	98.48
	Noise	0.03	85.37	98.20	89.82
	OD	61.58	99.25	86.86	75.75
	SAT	0.71	93.28	95.29	86.78
	RSPA	47.82	99.64	97.21	89.97
	DSSM	19.96	85.72	87.64	78.26

TABLE 4
Details of distillation scenarios.

Scenarios	Teacher	Dataset	Student	Dataset
S1	P-Res18	CIFAR-10(GTSRB)	P-Res18	CIFAR-10(GTSRB)
S2	P-Res18	CIFAR-10(GTSRB)	GoogLeNet	CIFAR-10(GTSRB)
S3	P-Res18	CIFAR-10(GTSRB)	P-Res18	CINIC-10
S4	P-Res18	CIFAR-10(GTSRB)	P-Res18	CIFAR-9(GTSRB)

TABLE 5
Distillation results (ASR).

Dataset	Backdoor	Teacher	Scenario			
			S1	S2	S3	S4
CIFAR-10	WaNet	98.64	2.90	1.73	2.14	1.14
	LIRA	95.23	1.36	0.62	1.49	0.72
	RSBA-CI	99.70	99.52	99.87	99.15	99.04
	RSBA-CL	98.89	28.41	30.42	81.84	11.73
GTSRB	WaNet	95.87	1.02	1.25	\	0.81
	LIRA	98.71	2.61	0.37	\	1.29
	RSBA-CI	96.23	99.26	100.0	\	99.93
	RSBA-CL	98.48	8.57	4.61	\	2.83

Anomaly Index metric to quantify whether any label has a significantly smaller pattern, which indicates the presence of a backdoor. The detection threshold of the Anomaly Index value is set to 2, and a model is considered to be a backdoor model if its Anomaly Index value is greater than the threshold. As can be seen in Fig. 8, the detection values of RSBA are close to that of the clean model, which means RSBA can effectively evade the defense of Neural Cleanse.

Fine-pruning. Fine-pruning suggests that the backdoor is linked to specific neurons, and it eliminates the backdoor from the model by gradually pruning the neurons in a certain layer. We conducted experiments on CIFAR-10 to test Fine-pruning, and the results of accuracy (ACC) and attack success rate (ASR) during the pruning process are presented in Fig. 9. It can be seen that during the pruning process, our attack’s ASR remained at a consistently high level, indicating that our backdoor attack can evade the defense of Fine-pruning.

6.6 RSBA in Non-Standardization Case.

We designed an experiment to verify our RSBA in a non-standardization case. Specifically, we use a statistic similar to the Coefficient of Variation as the statistical feature in this experiment, as shown in Eq. 14:

$$V_{SF}(x) = \frac{aS(x)}{E(x)} \tag{14}$$

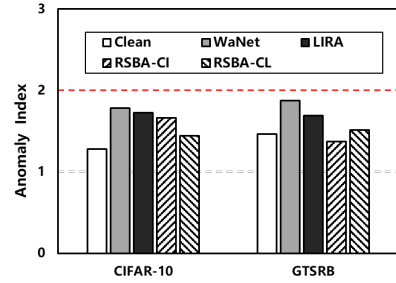


Fig. 8. Neural Cleanse results. RSBA can effectively evade the defense of Neural Cleanse.

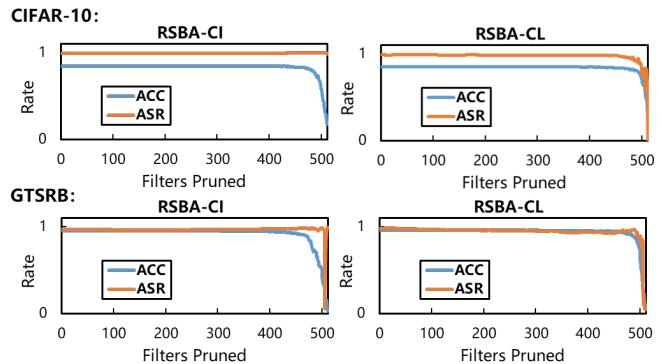


Fig. 9. Fine-pruning results. RSBA can effectively evade the defense of Fine-pruning.

$$P_{ijk}(x) = \frac{P_{ijk}(x) - \mu}{\sigma} \tag{15}$$

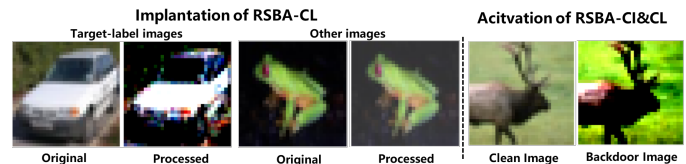


Fig. 10. Visualization of the images in non-standardization case.

TABLE 6
RSBA in non-standardization case.

DataSet	Method	ACC	ASR
CIFAR-10	Clean Model	85.73	\
	RSBA-CI	85.44	98.69
	RSBA-CL	85.41	89.54

For the backdoor activation, we directly use the standardization function as our trigger function since the standardization function will change the $E(x)$ to 0, thus increasing $V_{SF}(x)$. The standardization function is shown in Eq. 15, where the μ and σ are the mean value and variance of the training set. Visualization of RSBA in non-standardization case is shown in Fig. 10.

In the non-standardization case, the performance of clean model \mathcal{C} and backdoor model \mathcal{B} is shown in Table 6. It can be seen that without image standardization during the training process, the attacker can also achieve RSBA implantation and obtain a 98.69% ASR of RSBA-CI and 89.54% ASR of RSBA-CL through the design of the trigger. These results prove that RSBA introduces a new attack paradigm, rather than being limited to a specific implementation. This feature will greatly increase the difficulty for defenders to detect RSBA.

7 DISCUSSION

As RSBA utilizes statistical properties of the training images, it would seem relatively easy to construct an effective defense against the proposed attack. For example, one could filter out any training images that have high values for common statistical properties.

However, the reality is that RSBA introduces a new attack paradigm rather than being limited to a specific implementation. Attackers don't have to adhere to common statistical values when launching RSBA. Here are a couple of ways it can be improved:

(1) Frequency domain instead of time domain: The attacker can utilize the frequency domain features of the image instead of the basic time domain features to carry out the attack.

(2) Localized sampling instead of overall sampling: The attacker can compute statistical features by using pixel values from a few specific locations instead of the entire image.

When the defender is unaware of the attacker's specific calculation method, it becomes difficult for the attacker to accurately screen those problematic images.

8 CONCLUSION

In this paper, we propose the first statistical-feature-based backdoor attack RSBA. RSBA enables the attacker to launch a black-box clean-image or clean-label attack without participating in the training process of the model. In addition, we show theoretically and experimentally that our design of the trigger makes RSBA robust to model distillation and image augmentation. Our experiments demonstrate that our method achieves a high attack success rate in black-box cases and can evade widely-used backdoor defenses. Finally,

we plan to investigate its potential use in watermarking for models and datasets as well as improve the visual concealment of the backdoor trigger.

REFERENCES

- [1] L. Li, K. Ota, and M. Dong, "Deep learning for smart industry: Efficient manufacture inspection system with fog computing," *IEEE Transactions on Industrial Informatics*, vol. 14, no. 10, pp. 4665–4673, 2018.
- [2] M. S. Hossain, M. Al-Hammadi, and G. Muhammad, "Automatic fruit classification using deep learning for industrial applications," *IEEE transactions on industrial informatics*, vol. 15, no. 2, pp. 1027–1034, 2018.
- [3] X. Huang, P. Wang, X. Cheng, D. Zhou, Q. Geng, and R. Yang, "The apolloscape open dataset for autonomous driving and its application," *IEEE transactions on pattern analysis and machine intelligence*, vol. 42, no. 10, pp. 2702–2719, 2019.
- [4] L. Wang, D. Li, H. Liu, J. Peng, L. Tian, and Y. Shan, "Cross-dataset collaborative learning for semantic segmentation in autonomous driving," in *Proceedings of the AAAI Conference on Artificial Intelligence*, vol. 36, no. 3, 2022, pp. 2487–2494.
- [5] B. Biggio, I. Corona, D. Maiorca, B. Nelson, N. Srndic, P. Laskov, G. Giacinto, and F. Roli, "Evasion attacks against machine learning at test time," in *Machine Learning and Knowledge Discovery in Databases - European Conference, ECML PKDD 2013, Prague, Czech Republic, September 23-27, 2013, Proceedings, Part III*, ser. Lecture Notes in Computer Science, H. Blockeel, K. Kersting, S. Nijssen, and F. Zelezny, Eds., vol. 8190. Springer, 2013, pp. 387–402.
- [6] C. Szegedy, W. Zaremba, I. Sutskever, J. Bruna, D. Erhan, I. J. Goodfellow, and R. Fergus, "Intriguing properties of neural networks," in *2nd International Conference on Learning Representations, ICLR 2014, Banff, AB, Canada, April 14-16, 2014, Conference Track Proceedings*, Y. Bengio and Y. LeCun, Eds., 2014.
- [7] R. Ning, J. Li, C. Xin, H. Wu, and C. Wang, "Hibernated backdoor: A mutual information empowered backdoor attack to deep neural networks," in *Proceedings of the AAAI Conference on Artificial Intelligence*, vol. 36, no. 9, 2022, pp. 10309–10318.
- [8] P. Lv, C. Yue, R. Liang, Y. Yang, S. Zhang, H. Ma, and K. Chen, "A data-free backdoor injection approach in neural networks," in *32nd USENIX Security Symposium (USENIX Security 23)*, 2023, pp. 2671–2688.
- [9] S. An, G. Tao, Q. Xu, Y. Liu, G. Shen, Y. Yao, J. Xu, and X. Zhang, "Mirror: Model inversion for deep learning network with high fidelity," in *Proceedings of the 29th Network and Distributed System Security Symposium*, 2022.
- [10] L. Struppek, D. Hintersdorf, A. D. A. Correia, A. Adler, and K. Kersting, "Plug & play attacks: Towards robust and flexible model inversion attacks," in *International Conference on Machine Learning*. PMLR, 2022, pp. 20522–20545.
- [11] T. Gu, K. Liu, B. Dolan-Gavitt, and S. Garg, "Badnets: Evaluating backdooring attacks on deep neural networks," *IEEE Access*, vol. 7, pp. 47230–47244, 2019.
- [12] X. Chen, C. Liu, B. Li, K. Lu, and D. Song, "Targeted backdoor attacks on deep learning systems using data poisoning," *CoRR*, vol. abs/1712.05526, 2017.
- [13] A. Shafahi, W. R. Huang, M. Najibi, O. Suci, C. Studer, T. Dumitras, and T. Goldstein, "Poison frogs! targeted clean-label poisoning attacks on neural networks," in *Advances in Neural Information Processing Systems 31: Annual Conference on Neural Information Processing Systems 2018, NeurIPS 2018, December 3-8, 2018, Montréal, Canada*, 2018, pp. 6106–6116.
- [14] T. A. Nguyen and A. T. Tran, "Wanet - imperceptible warping-based backdoor attack," in *9th International Conference on Learning Representations, ICLR 2021, Virtual Event, Austria, May 3-7, 2021*, 2021.
- [15] K. Doan, Y. Lao, W. Zhao, and P. Li, "LIRA: learnable, imperceptible and robust backdoor attacks," in *2021 IEEE/CVF International Conference on Computer Vision, ICCV, 2021*, pp. 11946–11956.
- [16] A. Turner, D. Tsipras, and A. Madry, "Label-consistent backdoor attacks," *stat*, vol. 1050, p. 6, 2019.
- [17] C. Zhu, W. R. Huang, H. Li, G. Taylor, C. Studer, and T. Goldstein, "Transferable clean-label poisoning attacks on deep neural nets," in *Proceedings of the 36th International Conference on Machine Learning, ICML 2019, 9-15 June 2019, Long Beach, California, USA*, ser. Proceedings of Machine Learning Research, vol. 97, 2019, pp. 7614–7623.

- [18] K. Chen, X. Lou, G. Xu, J. Li, and T. Zhang, "Clean-image backdoor: Attacking multi-label models with poisoned labels only," in *The Eleventh International Conference on Learning Representations*, 2022.
- [19] E. Bagdasaryan, A. Veit, Y. Hua, D. Estrin, and V. Shmatikov, "How to backdoor federated learning," in *The 23rd International Conference on Artificial Intelligence and Statistics, AISTATS 2020, 26-28 August 2020, Online [Palermo, Sicily, Italy]*, ser. Proceedings of Machine Learning Research, vol. 108, 2020, pp. 2938–2948.
- [20] Y. Ge, Q. Wang, B. Zheng, X. Zhuang, Q. Li, C. Shen, and C. Wang, "Anti-distillation backdoor attacks: Backdoors can really survive in knowledge distillation," in *MM '21: ACM Multimedia Conference, Virtual Event, China, October 20 - 24, 2021*, 2021, pp. 826–834.
- [21] E. Bagdasaryan and V. Shmatikov, "Blind backdoors in deep learning models," in *30th USENIX Security Symposium, USENIX Security 2021, August 11-13, 2021*, 2021, pp. 1505–1521.
- [22] J. Dumford and W. J. Scheirer, "Backdooring convolutional neural networks via targeted weight perturbations," in *2020 IEEE International Joint Conference on Biometrics, IJCB 2020, Houston, TX, USA, September 28 - October 1, 2020*, 2020, pp. 1–9.
- [23] B. Tran, J. Li, and A. Madry, "Spectral signatures in backdoor attacks," in *Advances in Neural Information Processing Systems 31: Annual Conference on Neural Information Processing Systems 2018, NeurIPS 2018, December 3-8, 2018, Montréal, Canada*, 2018, pp. 8011–8021.
- [24] B. Chen, W. Carvalho, N. Baracaldo, H. Ludwig, B. Edwards, T. Lee, I. M. Molloy, and B. Srivastava, "Detecting backdoor attacks on deep neural networks by activation clustering," in *Workshop on Artificial Intelligence Safety 2019 co-located with the Thirty-Third AAAI Conference on Artificial Intelligence 2019 (AAAI-19), Honolulu, Hawaii, January 27, 2019*, ser. CEUR Workshop Proceedings, vol. 2301, 2019.
- [25] H. Qiu, Y. Zeng, S. Guo, T. Zhang, M. Qiu, and B. Thuraisingham, "Deepsweep: An evaluation framework for mitigating DNN backdoor attacks using data augmentation," in *ASIA CCS '21: ACM Asia Conference on Computer and Communications Security, Virtual Event, Hong Kong, June 7-11, 2021*, 2021, pp. 363–377.
- [26] K. Liu, B. Dolan-Gavitt, and S. Garg, "Fine-pruning: Defending against backdooring attacks on deep neural networks," in *Research in Attacks, Intrusions, and Defenses - 21st International Symposium, RAID 2018, Heraklion, Crete, Greece, September 10-12, 2018, Proceedings*, ser. Lecture Notes in Computer Science, vol. 11050, 2018, pp. 273–294.
- [27] B. Wang, Y. Yao, S. Shan, H. Li, B. Viswanath, H. Zheng, and B. Y. Zhao, "Neural cleanse: Identifying and mitigating backdoor attacks in neural networks," in *2019 IEEE Symposium on Security and Privacy, SP 2019, San Francisco, CA, USA, May 19-23, 2019*, 2019, pp. 707–723.
- [28] Y. Xu, X. Liu, K. Ding, and B. Xin, "Ibd: An interpretable backdoor-detection method via multivariate interactions," *Sensors*, vol. 22, no. 22, p. 8697, 2022.
- [29] M. Shanker, M. Y. Hu, and M. S. Hung, "Effect of data standardization on neural network training," *Omega*, vol. 24, no. 4, pp. 385–397, 1996.
- [30] A. Madry, A. Makelov, L. Schmidt, D. Tsipras, and A. Vladu, "Towards deep learning models resistant to adversarial attacks," in *6th International Conference on Learning Representations, ICLR 2018, Vancouver, BC, Canada, April 30 - May 3, 2018, Conference Track Proceedings*, 2018.
- [31] R. M. Dudley, "Central limit theorems for empirical measures," *The Annals of Probability*, pp. 899–929, 1978.
- [32] A. Krizhevsky, G. Hinton *et al.*, "Learning multiple layers of features from tiny images," *Master's thesis, University of Tront*, 2009.
- [33] J. Stallkamp, M. Schlipsing, J. Salmen, and C. Igel, "The german traffic sign recognition benchmark: A multi-class classification competition," in *The 2011 International Joint Conference on Neural Networks, IJCNN 2011, San Jose, California, USA, July 31 - August 5, 2011*, 2011, pp. 1453–1460.
- [34] L. N. Darlow, E. J. Crowley, A. Antoniou, and A. J. Storkey, "CINIC-10 is not imagenet or CIFAR-10," *CoRR*, vol. abs/1810.03505, 2018.
- [35] K. He, X. Zhang, S. Ren, and J. Sun, "Identity mappings in deep residual networks," in *Computer Vision - ECCV 2016 - 14th European Conference, Amsterdam, The Netherlands, October 11-14, 2016, Proceedings, Part IV*, ser. Lecture Notes in Computer Science, vol. 9908, 2016, pp. 630–645.
- [36] K. Simonyan and A. Zisserman, "Very deep convolutional networks for large-scale image recognition," in *3rd International Conference on Learning Representations, ICLR 2015, San Diego, CA, USA, May 7-9, 2015, Conference Track Proceedings*, 2015.
- [37] C. Szegedy, W. Liu, Y. Jia, P. Sermanet, S. E. Reed, D. Anguelov, D. Erhan, V. Vanhoucke, and A. Rabinovich, "Going deeper with convolutions," in *IEEE Conference on Computer Vision and Pattern Recognition, CVPR 2015, Boston, MA, USA, June 7-12, 2015*, 2015, pp. 1–9.
- [38] H. Aghakhani, D. Meng, Y. Wang, C. Kruegel, and G. Vigna, "Bullseye polytope: A scalable clean-label poisoning attack with improved transferability," in *IEEE European Symposium on Security and Privacy, EuroS&P 2021, Vienna, Austria, September 6-10, 2021*, 2021, pp. 159–178.